

A leading order imaging series for prestack data acquired over a laterally invariant acoustic medium: Analysis for bandlimited input data

Simon A. Shaw and Arthur B. Weglein, University of Houston

Summary

We are using the inverse scattering series, a multidimensional direct inversion procedure, to derive an algorithm that can accurately depth image seismic data directly in terms of an inaccurate velocity. Previously, a subseries of the inverse series had been isolated (for a 1D normal incidence experiment in an acoustic medium) that moves reflectors towards their correct spatial location using the inadequate reference velocity. Here, this imaging series algorithm is formulated for an experiment in which a point source explodes in a three-dimensional constant density acoustic medium where the velocity varies only in depth, thereby confining our current study to the positioning of reflectors vertically.

The imaging series is a cascaded series in that every term is itself an infinite series in the recorded data. The leading order imaging series consists of the portion of each term that is leading order in the data and is therefore an approximation to the full depth imaging potential of the inverse series. It has been found to converge for large contrasts between the actual and reference medium. The first term locates reflectors at the depths dictated by the reference velocity and the data's travel times. The remaining terms use the data's amplitudes and travel times to shift the reflectors closer to their correct location.

Analytic and bandlimited numerical examples demonstrate that the leading order imaging series improves the predicted depths of the reflectors at precritical angles, acting to flatten the angle gathers. We use synthetic reflectivity data examples to show that, even when missing zero and low temporal frequency information, the leading order imaging series locates reflectors closer to their actual depths than a migration with the reference velocity. For higher contrasts, or when greater accuracy is desired, then higher order imaging terms are required.

Introduction and background

Current depth imaging algorithms can be formulated from a linear inverse scattering model, in which the reference velocity is assumed to be close enough to the actual velocity in order to place reflectors at their correct spatial locations. In practice, especially in complex geological environments, methods for deriving the reference velocity model can be inadequate for linear imaging algorithms inasmuch as they fail to focus reflectors at their correct locations. The inverse scattering series has the ability to image primary reflection events at their correct location using only the reflection data and an approximate velocity model (Weglein et al., 2000). The first term in the inverse series is a linear inversion of the data. Using a velocity model that is incorrect below the

measurement surface, the first term will locate primaries at locations expected when imaging with a conventional algorithm. Therefore, the first term in the series will mislocate reflectors unless the velocity model is correct. The higher order terms in the inverse series, that are non-linear in the data, contain parts that move the reflectors to their true spatial locations. These terms are non-zero when the velocity model is incorrect.

As a multidimensional direct inversion procedure (Moses, 1956), the inverse series removes multiples, locates reflectors, and inverts amplitudes for medium parameters *directly* using only the measured data and a reference medium's parameters. Adopting the strategy of isolating task-specific subseries described by Weglein et al. (2003), we assume that free-surface and internal multiples have been removed (Weglein et al., 1997), and the source wavelet is known (a prerequisite for all inverse series algorithms). Our objective is to locate reflectors in space (not invert for changes in earth material properties).

Shaw et al. (2003) considered the simplest case of a normal-incidence experiment over a 1D constant density acoustic medium for which the velocity was an unknown function of depth. An imaging series algorithm was derived that images reflectors in depth using a constant reference velocity and it was shown analytically that this series converges for large finite contrasts between the actual and reference velocities. For relatively small contrasts, the leading order imaging series is a good approximation to the entire imaging series in that the predicted depths are a significant improvement over conventional depth imaging with the reference velocity. It was also demonstrated that this series converges more rapidly for smaller contrasts and for lower maximum frequencies. Therefore, a proximate reference velocity and a source spectrum with a lower maximum frequency aid the rate of convergence.

Having established for the simplest case that the leading order imaging series has good convergence properties, the next step in developing a practical algorithm is to evaluate its efficacy under increasingly realistic conditions. Since seismic data are always bandlimited, one of the highest priority tests is an analysis of the algorithm under conditions of missing low frequencies. With this objective, we retain the simplicity of the acoustic model, but rederive the leading order imaging series to accommodate prestack input data which provide a lower vertical wavenumber more closely mirroring the actual experiment.

We present analytic and bandlimited synthetic examples of a prestack leading order imaging series. The analytic examples show how the algorithm performs depth imaging given a constant reference velocity that is never updated. The synthetic examples demonstrate that the algorithm retains effectiveness even when missing low frequencies.

Leading order imaging series

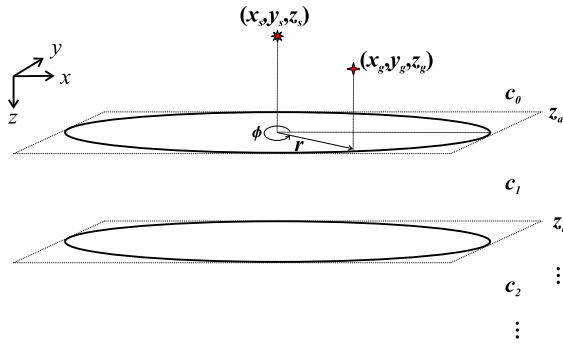


Fig. 1: A multi-layer 1D constant density acoustic model.

For a 3D constant density acoustic medium with point sources and receivers located at $\vec{x}_s = (x_s, y_s, z_s)$ and $\vec{x}_g = (x_g, y_g, z_g)$, respectively (see Fig. 1), wave propagation is characterized by

$$\left(\nabla^2 + \frac{\omega^2}{c^2(\vec{x}_g)}\right) \tilde{P}(\vec{x}_g|\vec{x}_s; \omega) = -A(\omega)\delta(\vec{x}_g - \vec{x}_s) \quad (1)$$

where \tilde{P} is the pressure field, A is the source wavelet, c is the propagation velocity and ω is the angular frequency. To simplify the current analysis, we assume that the medium varies only in the z direction. For the generalization to a 2D earth, see Fang et al. (2004). The velocity, c , can be expressed in terms of a constant reference velocity, c_0 , and a perturbation, α , such that

$$1/c^2(z) = [1 - \alpha(z)]/c_0^2. \quad (2)$$

The goal of inversion is to solve for α which is written

$$\alpha = \alpha_1 + \alpha_2 + \alpha_3 + \dots \quad (3)$$

where α_1 , the first term in the series for α , is linearly related to the measured scattered field, $\tilde{P}_s = \tilde{P} - \tilde{P}_0$. \tilde{P}_0 is the pressure wavefield due to the same source, $A(\omega)$, in the reference medium chosen to be a wholespace with velocity c_0 . The second term is quadratic in \tilde{P}_s , the third term is cubic and so on. After using the inverse series to solve for α , we could use (2) to solve for the velocity, c . However, our objective is not to solve for the medium parameters, but to solve directly for the *location* at which α changes. This is the problem of imaging in a medium whose velocity is not known before or after the imaging procedure.

A prestack leading order imaging series

The inverse series equations are

$$\tilde{D} = G_0 V_1 G_0 \quad (4)$$

$$G_0 V_2 G_0 = -G_0 V_1 G_0 V_1 G_0 \quad (5)$$

$$G_0 V_3 G_0 = -G_0 V_1 G_0 V_1 G_0 V_1 G_0 - G_0 V_1 G_0 V_2 G_0 - G_0 V_2 G_0 V_1 G_0 \quad (6)$$

⋮

where, for the acoustic medium considered here, $V_n = k_0^2 \alpha_n$, $k_0 = \omega/c_0$ and G_0 is the causal Green's function satisfying the wave equation in the reference medium. In (4), \tilde{D} is the scattered field evaluated on the measurement surface and the source wavelet has been deconvolved so $\tilde{D} = \tilde{P}_s/A$. Hence, \tilde{D} is related to α_1 by

$$\tilde{D}(\vec{x}_g|\vec{x}_s; \omega) = \int_{-\infty}^{+\infty} G_0(\vec{x}_g|\vec{x}'; \omega) k_0^2 \alpha_1(z') G_0(\vec{x}'|\vec{x}_s; \omega) d\vec{x}' \quad (7)$$

and the solution for α_1 in cylindrical coordinates is

$$\tilde{\alpha}_1(-2q_g) = 2\pi \frac{-Aq_g^2}{k_0^2} e^{iq_g z_m} \int_0^{+\infty} \tilde{D}(r; \omega) J_0(k_r r) r dr \quad (8)$$

where $z_m = z_g + z_s$ and the vertical and horizontal wavenumbers, q_g and k_r , respectively, are related by

$$q_g = k_0 \sqrt{1 - k_r^2/k_0^2}. \quad (9)$$

$J_0(k_r r)$ is a zero order Bessel function of the first kind that arises due to the azimuthal symmetry. The fact that the data are a function of both time and source-receiver offset whereas α is only a function of depth is evident in (8) in that $\tilde{\alpha}_1$ is over-determined. Considering fixed angles of incidence, θ_0 , leads to a number of different estimates of α_1 , denoted by $\alpha_1(z, \theta_0)$. Fixing θ_0 is the same as fixing horizontal and vertical slownesses, p_0 and ζ_0 , respectively:

$$p_0 = (\sin \theta_0)/c_0 \text{ and } \zeta_0 = (\cos \theta_0)/c_0.$$

However, q_g is still allowed to vary through the variation in ω since $q_g = \omega \zeta_0$. Proceeding with this choice and inverse Fourier transforming both sides of (8) gives

$$\alpha_1(z, \theta_0) = -8\zeta_0 \cos^2 \theta_0 \times \int_{-\infty}^{+\infty} e^{-i\omega\tau} \int_0^{+\infty} \tilde{D}(r; \omega) J_0(\omega p_0 r) r dr d\omega. \quad (10)$$

where $\tau = \zeta_0(2z - z_m)$. Equation (10) is a scaled slant stack of the recorded data. An alternative approach to handling the degree of freedom is to hold ω fixed and integrate over angle or vertical slowness. This parameterization will result in different estimates of α_1 for constant ω values and is the subject of ongoing research.

The imaging series is a subseries of the inverse series that positions reflectors at their correct spatial location (Weglein et al., 2002). For the problem in which the earth is characterized by a single parameter, the imaging series is

$$\alpha^{\text{IM}} = \alpha_1^{\text{IM}} + \alpha_2^{\text{IM}} + \alpha_3^{\text{IM}} + \dots \quad (11)$$

where α_n^{IM} is the term in the imaging series that is n^{th} order in the measured field and is found in the n^{th} term of the inverse series. α^{IM} is a cascaded series in that each term is itself and infinite series in the data. The leading order imaging series, α^{LOIM} , is the contribution to

Leading order imaging series

the imaging series that is leading order in the data. The terms in this imaging series have been found to exhibit a specific pattern (corresponding to particular inverse scattering diagrams) recognized by Shaw et al. (2003) allowing the prediction of a general form. Using the constant- θ_0 formulation, the prestack form of the algorithm is

$$\alpha^{\text{LOIM}}(z, \theta_0) = \sum_{n=0}^{\infty} \frac{(-1/2)^n}{n! \cos^{2n} \theta_0} \left(\int_0^z \alpha_1(z', \theta_0) dz' \right)^n \times \frac{\partial^n \alpha_1(z, \theta_0)}{\partial z^n} \quad (12)$$

where $\alpha_1(z, \theta_0)$ is given by (10). There is a closed form for the 1D leading order imaging series:

$$\alpha^{\text{LOIM}}(z, \theta_0) = \alpha_1 \left(z - \frac{1/2}{\cos^2 \theta_0} \int_0^z \alpha_1(z', \theta_0) dz', \theta_0 \right). \quad (13)$$

The rate of convergence of (12) is greater for smaller values of k_z , smaller values of $\int_0^z \alpha_1(z', \theta_0) dz'$, and smaller values of θ_0 . Analysis of the 1D normal incidence algorithm showed that, for relatively small contrasts (the actual velocity within about 10% of the reference velocity), the leading order contributions to the imaging series can accurately locate reflectors. Higher contrasts or greater accuracy require higher order imaging terms.

Analytic and bandlimited numerical examples

Consider a model that consists of two horizontal interfaces at depths z_a and z_b (Fig. 1). For this example,

$$\tilde{D}(r; \omega) = - \int_0^{+\infty} \frac{(R_{01} + R'_{12} e^{2i\omega\zeta_1(z_b - z_a)})}{i\omega\zeta_0} \times e^{i\omega\zeta_0(2z_a - z_m)} J_0(k_r r) k_r dk_r \quad (14)$$

where the amplitudes are functions of angle and are

$$R_{01} = \frac{\zeta_0 - \zeta_1}{\zeta_0 + \zeta_1} \text{ and } R'_{12} = \frac{-2\zeta_1}{\zeta_0 + \zeta_1} \frac{\zeta_1 - \zeta_2}{\zeta_1 + \zeta_2} \frac{2\zeta_0}{\zeta_0 + \zeta_1} \quad (15)$$

and

$$\zeta_i = (\cos \theta_i) / c_i, \quad i = 0, 1, 2, \dots \quad (16)$$

Substituting the data (14) into the linear inverse equation (10), then for this two-reflector example, the first term in the series for $\alpha(z)$ can be written as a function of angle

$$\alpha_1(z, \theta_0) = 4 \cos^2 \theta_0 [R_{01} H(z - z_a) + R'_{12} H(z - z_b)] \quad (17)$$

where the shallower reflector is correctly located at z_a (since the velocity down to z_a was correct) but the deeper reflector is mislocated at depth

$$z_{b'} = z_a + (z_b - z_a) \frac{\zeta_1}{\zeta_0}. \quad (18)$$

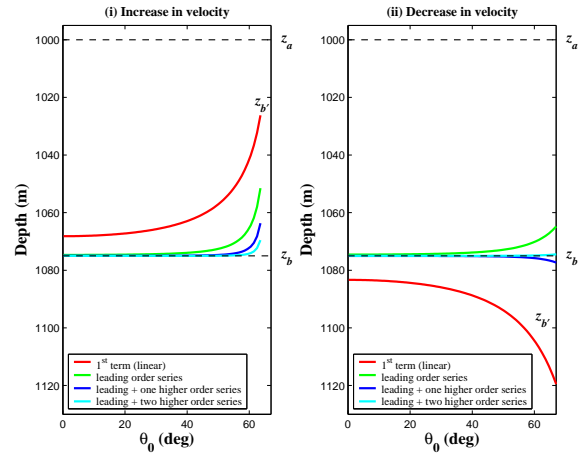


Fig. 2: Depths predicted by the first term in the series and three different imaging series as a function of angle for two analytic examples: $z_a = 1000$ m, $z_b = 1075$ m, $c_0 = 1500$ m/sec and $c_1 = 1650$ m/s (i), $c_1 = 1350$ m/sec (ii).

The shift of the deeper reflector to its correct depth can be written as an infinite series in the data:

$$z_b - z_{b'} = -2(z_{b'} - z_a) (R_{01} - R_{01}^2 + R_{01}^3 - \dots) \quad (19)$$

under the condition that $|R_{01}| < 1$, which precludes post-critical reflections. The approximation to this shift that is leading order in the scattered field is

$$z_b - z_{b'} \approx -2(z_{b'} - z_a) R_{01}. \quad (20)$$

This is equal to the shift calculated by the leading order imaging series. To see this, we substitute the first term in the imaging series for this example (17) into the closed form for α^{LOIM} (13) and evaluate the algorithm at z_b :

$$\alpha^{\text{LOIM}}(z_b, \theta_0) = \alpha_1(z_b, \theta_0) - 2(z_b - z_a) R_{01}(\theta_0). \quad (21)$$

Hence, the leading order imaging series α^{LOIM} shifts the interface at $z_{b'}$ in α_1 to a depth $z_{b'} + 2(z_b - z_a) R_{01}$ which is closer to the actual depth z_b and is a function of angle. The leading order imaging series, α^{LOIM} , is a better approximation to the entire imaging series, α^{IM} , when the magnitude of the perturbation above the reflector being imaged is smaller. Higher order imaging terms include successively more amplitude terms in the series for the shift in (19). For models containing more than two interfaces, the leading order imaging series produces an approximation to the shift at each mislocated interface that is an infinite series in reflection and transmission coefficients in the overburden.

Figure 2 shows two analytic examples where the reference velocity $c_0 = 1500$ m/sec and two reflectors are located at $z_a = 1000$ m and $z_b = 1075$ m. The depths predicted by the first term in the series and three approximations to the imaging series are displayed. The variation of $z_{b'}$ with angle is the residual moveout resulting from a migration with the incorrect (reference) velocity. Figure 2

Leading order imaging series

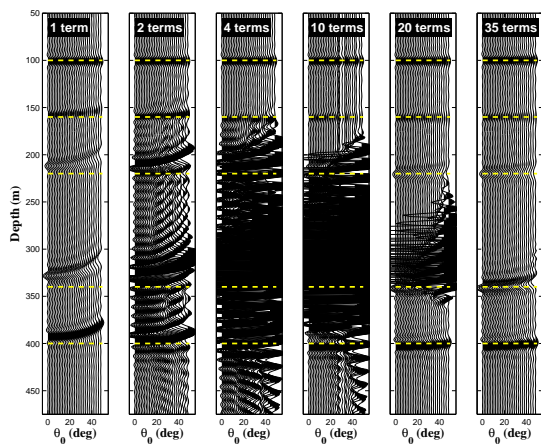


Fig. 3: Cumulative sum of up to 35 terms in the prestack leading order imaging series (Eq. 12) for a 6-layer model. The yellow dashed lines are the actual depths of the reflectors. The first term is a migration with the constant reference velocity.

shows that including higher order imaging terms improves the accuracy of the predicted depth, especially at higher angles where they are needed more. Figure 3 shows the cumulative sum of up to 35 terms in the leading order imaging series (Eq. 12) for a 6-layer model. In this case, after 35 terms the series has converged. Finally, Fig. 4 shows that the algorithm retains effectiveness even when missing zero and low frequencies.

Conclusions

We have reformulated the prestack imaging series for a 1D medium and for a point-source experiment, and have demonstrated its effectiveness on analytic and bandlimited numerical examples. This prestack formulation, and its effectiveness with band-limited data, motivate continued progression towards its generalization for eventual field data application, which is further encouraged by the current industry trend towards lower frequency acquisition.

Acknowledgements

ConocoPhillips (Hugh Rowlett and Rob Habiger) are thanked for their financial support of S. A. Shaw and for their encouragement of this research. The support of Ken Matson and Gerhard Pfau at BP, Dennis Corrigan, Bogdan Nita, Kris Innanen, Einar Otnes and the sponsors of M-OSRP is gratefully acknowledged.

References

- Fang, L., B. G. Nita, A. B. Weglein, and K. A. Innanen (2004). Inverse scattering series in the presence of lateral variations. *M-OSRP Annual Report 3*, 182–204.
- Moses, H. (1956). Calculation of scattering potential from reflection coefficients. *Phys. Rev.* (102), 559–567.

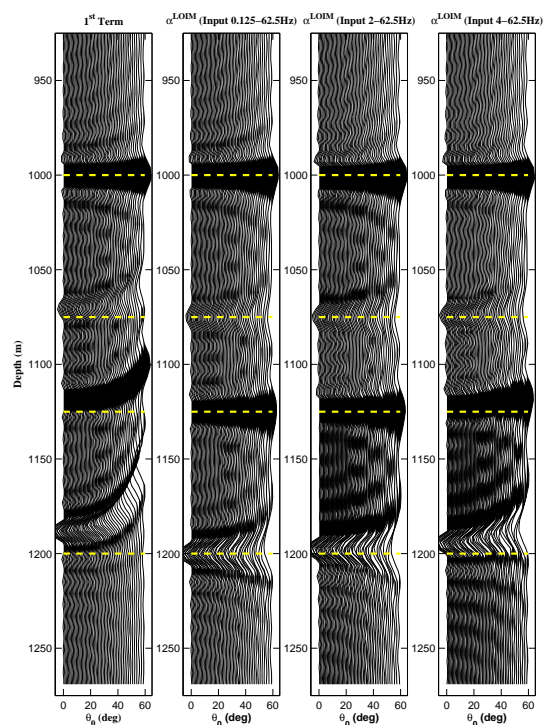


Fig. 4: The leading order imaging series for a range of band-limited input data.

Shaw, S. A., A. B. Weglein, D. J. Foster, K. H. Matson, and R. G. Keys (2003). Isolation of a leading order depth imaging series and analysis of its convergence properties. In *73rd Annual Internat. Mtg., Soc. Expl. Geophys., Expanded Abstracts*. Soc. Expl. Geophys.

Weglein, A. B., F. V. Araújo, P. M. Carvalho, R. H. Stolt, K. H. Matson, R. T. Coates, D. Corrigan, D. J. Foster, S. A. Shaw, and H. Zhang (2003). Inverse scattering series and seismic exploration. *Inverse Problems 19*, R27–R83.

Weglein, A. B., D. J. Foster, K. H. Matson, S. A. Shaw, P. M. Carvalho, and D. Corrigan (2002). Predicting the correct spatial location of reflectors without knowing or determining the precise medium and wave velocity: initial concept, algorithm and analytic and numerical example. *Journal of Seismic Exploration 10*, 367–382.

Weglein, A. B., F. A. Gasparotto, P. M. Carvalho, and R. H. Stolt (1997). An inverse-scattering series method for attenuating multiples in seismic reflection data. *Geophysics 62*(6), 1975–1989.

Weglein, A. B., K. H. Matson, D. J. Foster, P. M. Carvalho, D. Corrigan, and S. A. Shaw (2000). Imaging and inversion at depth without a velocity model: Theory, concepts and initial evaluation. In *70th Annual Internat. Mtg., Soc. Expl. Geophys., Expanded Abstracts*, pp. 1016–1019. Soc. Expl. Geophys.